

基于吸收光谱技术的制冷剂膜厚测量系统研制

孔帅帅, 许晓妍, 孙昊, 方奕栋, 苏明旭, 杨荟楠*

上海理工大学能源与动力工程学院, 上海 200093

摘要 制冷剂液膜蒸发现象广泛地存在于航空航天、制冷空调和消费电子等领域, 高精度定量分析液膜厚度对于了解液膜分布情况、揭示液膜传热规律及优化相关工业过程至关重要。将 R1233zd 作为研究对象, 提出一种基于吸收光谱技术的制冷剂液膜厚度测量新方法。首先获取了不同温度(11.8, 13.5, 15.2, 16.5, 18.0 °C)下 R1233zd 的吸收光谱, 构建液膜厚度反演模型, 并研制膜厚测量系统。利用厚度可调(0~800 μm)的标准具对该系统的测量精度进行验证。进一步结合图像法对水平石英玻璃板上的 R1233zd 液膜蒸发过程进行研究, 发现两种方法测得的液膜厚度随时间的变化趋势吻合良好。该系统实现了 R1233zd 液膜蒸发过程中膜厚的高精度测量, 有望为相关工业过程的设计和优化提供数据支撑。

关键词 测量; 吸收光谱; 膜厚; 蒸发

中图分类号 TK31 **文献标志码** A

DOI: 10.3788/CJL202249.1704004

1 引言

制冷剂液膜蒸发现象广泛地存在于航空航天、制冷空调和消费电子等多个领域^[1-7]。液膜蒸发过程中膜厚与传热性能密切相关, 定量分析液膜厚度有助于了解传热规律, 为优化相关工业过程提供科学指导^[8-9]。国内外科研人员基于数值模拟的方法对制冷剂液膜进行了大量研究。Li 等^[10]利用湍流和相变模型对矩形微通道中制冷剂 R134a 的冷凝传热和流动特性进行了数值研究, 发现液膜厚度随着质量流量和蒸汽质量的降低而增大。蒋淳等^[11]通过建立三维模型对水平管外制冷剂 R410A 的降膜蒸发过程进行了模拟, 讨论了喷淋密度和热通量对液膜厚度和传热的影响。Sripattrapan 等^[12]通过建立环状流模型对双管蒸发器中不同热通量下制冷剂 R134a 的蒸发过程进行了研究, 分析了液膜厚度与传热系数的沿程变化规律。由于数值模拟往往建立在简化假设的基础上, 因此计算结果的可信度低。

近年来, 许多学者基于电学法^[13-15]、声学法^[16-17]和光学法^[18-21]对液膜厚度测量开展了大量的实验研究, 但与制冷剂液膜相关的工作鲜有报道。Klausner 等^[22]基于电容法对热交换器水平管内 R113 流动沸腾过程中环状流液膜厚度进行了测量, 但该方法仅适用于导电流体。Vergne 等^[23]利用光学干涉测量技术对

空调系统的压缩机中润滑轴承的 R123 液膜厚度进行了测量, 但测量精度严重依赖于液膜的流型, 因为液膜波动时光的反射和衍射均会受到影响。Martinez-Galván 等^[24]利用配有长工作距离显微镜的高速相机对喷雾冷却系统雾化过程中形成的 R134a 液膜进行了研究, 但该方法的测量精度受液膜边缘检测的影响。由此可见, 上述方法均具有一定的局限性, 无法实现对制冷剂液膜厚度无干扰和高精度的测量。

R1233zd 是一种臭氧消耗潜能值为零、全球变暖潜能值较低、不可燃的新型制冷剂^[25], 具有良好的环保性能。本文以 R1233zd 为研究对象, 提出一种具有普适性的无干扰、高精度制冷剂液膜厚度测量新方法。首先利用傅里叶变换红外光谱仪对不同温度下的 R1233zd 进行了长频域扫描, 构建了液膜厚度反演模型。在此基础上, 研制了基于吸收光谱技术的 R1233zd 液膜厚度测量系统, 利用厚度可调的标准具对该系统的测量精度进行了验证。并进一步对水平石英玻璃板上的 R1233zd 液膜蒸发过程进行了研究。

2 基本原理

2.1 R1233zd 吸收光谱

本文首先自制了用于不同温度下 R1233zd 吸收光谱测量研究的高精度温度控制装置。如图 1 所示, 利用热电偶测量石英比色皿中 R1233zd 的温度, 将其

收稿日期: 2021-12-06; 修回日期: 2021-12-27; 录用日期: 2022-01-06

基金项目: 国家自然科学基金(51676130)、上海市自然科学基金(20ZR1438900)

通信作者: *yanghuinan@usst.edu.cn

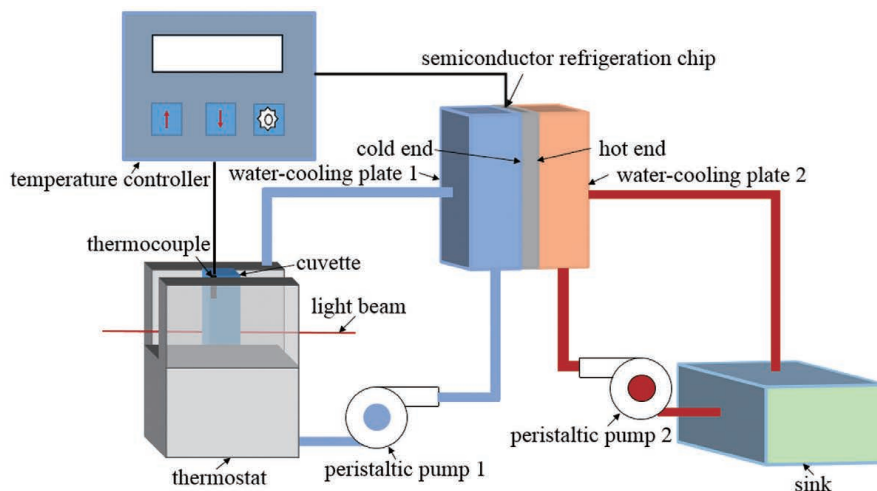


图1 自制温度控制装置

Fig. 1 Homemade temperature control device

与温度控制器所设的阈值进行比较,从而控制半导体制冷片的工作状态,达到对 R1233zd 精准控温 ($\pm 0.1\text{ }^{\circ}\text{C}$)的目的。R1233zd 的热量通过热传导的方式传输到恒温水浴中,恒温水浴中的水在蠕动泵 1 的作用下进入水冷板 1 中,制冷片冷端吸收水冷板 1 中水的热量。同时,为了防止制冷片热端热量渗透到冷端影响制冷效果,本文采用水冷散热方式提高制冷性能,水槽中的水在蠕动泵 2 的驱动下进入水冷板 2 中吸收制冷片热端的热量。

在此基础上,将 R1233zd 放置在光程为 2.0 mm 的石英比色皿中,利用高分辨率 (0.25 cm^{-1}) 的傅里叶变换红外光谱仪对其沸点 ($18.3\text{ }^{\circ}\text{C}$) 以下 5 个不同温度 ($T = 11.8, 13.5, 15.2, 16.5, 18.0\text{ }^{\circ}\text{C}$) 处的 R1233zd 进行长频域扫描,发现在近红外区域 ($5800.0\sim 6300.0\text{ cm}^{-1}$) 存在明显吸收,如图 2 所示。其中,最大吸收系数 (k) 对应的波数位置为 6076.5 cm^{-1} (虚线),在其附近, dk/dT 为零时对应的波数位置为 6080.5 cm^{-1} 。

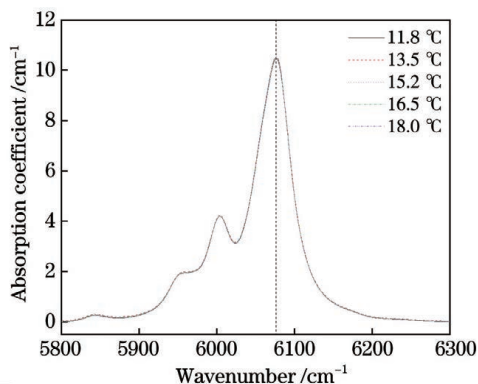


图2 近红外区域内不同温度下 R1233zd 的吸收光谱

Fig. 2 Absorption spectra of R1233zd at different temperatures in near infrared range

2.2 液膜厚度反演模型

基于比尔-朗伯定律,波数为 ν_i 的光束穿过吸收介质后透射率可表示为

$$\tau(\nu_i) = \frac{I_t}{I_0} = (1-u)\exp(k_{\nu_i}L), \quad (1)$$

式中: I_t 和 I_0 分别为透射光强和入射光强; L 为光程(液膜厚度); k_{ν_i} 为吸收介质在波数 ν_i 位置的吸收系数; i 为波数编号; u 为其他因素造成的光强衰减,如液膜表面反射和光路偏转等。本文优选两个波数位置进行研究,从而消除 u 对测量精度的影响。其中,在波数位置 ν_1 制冷剂吸收系数较大,在波数位置 ν_2 制冷剂吸收系数为零,且在这两个波数位置吸收系数几乎不受温度影响。

基于式(1),结合两个波数位置的透射率, L 可以表示为

$$L = \frac{\ln[\tau(\nu_1)/\tau(\nu_2)]}{k_{\nu_2} - k_{\nu_1}}. \quad (2)$$

本文以 R1233zd 为例,建立了基于比尔-朗伯定律的反演模型以高精度测量制冷剂液膜厚度。该方法也适用于其他种类的制冷剂,技术路线与本文相同。首先利用傅里叶变换红外光谱仪获取制冷剂的吸收光谱,通过优选波数位置,并结合液膜厚度反演模型,确定了制冷剂液膜厚度信息。

3 分析与讨论

3.1 测量系统研制及精度验证

本文研制了基于吸收光谱技术的制冷剂液膜厚度测量系统(图 3),该系统以卤钨灯作为光源,最大功率为 9.0 W ,输出波数范围为 $4000.0\sim 27777.0\text{ cm}^{-1}$ 的白光。白光经透镜准直后被滤光片过滤掉超出近红外光谱仪响应范围的光信号,再被凸透镜(焦距 $f = 15.0\text{ mm}$)聚焦后入射至液膜。经液膜透射后再经凸透镜聚焦到光纤端口,经光纤传输后被近红外光谱仪接收。近红外光谱仪将光信号转化为电信号,并传输至计算机,最后采用自编 LabVIEW 程序进行数据后处理。

基于 R1233zd 的吸收光谱和液膜厚度反演模型,

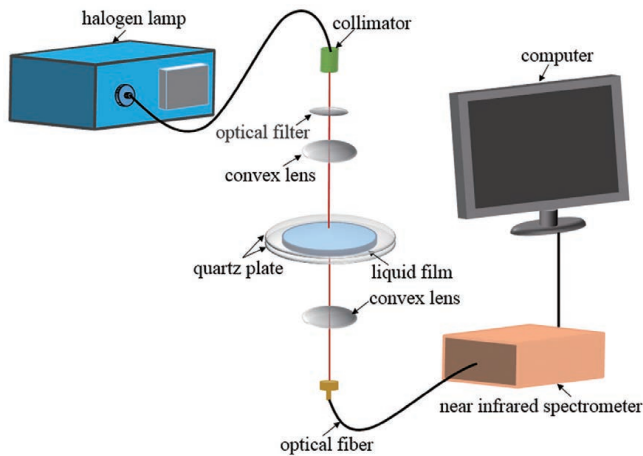


图3 研制的基于吸收光谱技术的测量系统

Fig. 3 Developed measurement system based on absorption spectroscopy

并结合分辨率为 5.2 cm^{-1} 的光谱仪,本文选取波数位置 ν_1 为 6080.5 cm^{-1} 附近的 6077.7 cm^{-1} , 波数位置

ν_2 为 6249.8 cm^{-1} , 此处吸收系数几乎为零。波数位置 ν_1 处的 dk/dT 为 $0.0007 \text{ cm}^{-1} \cdot \text{°C}^{-1}$, 经计算发现由温度波动 ($\pm 1 \text{ °C}$) 造成的液膜厚度测量误差小于 0.0067% 。为了尽量避免温度对测量精度的影响, 本文所有的实验研究都将温度控制在 13.5 °C 。

在此基础上, 首先利用液膜厚度可调 ($0 \sim 800 \text{ }\mu\text{m}$) 的标准具对该系统的测量精度进行验证, 即通过改变标准具中两块透明石英玻璃板的间距来实现液膜厚度变化。对标准具中 8 个不同厚度 ($100, 200, 300, 400, 500, 600, 700, 800 \text{ }\mu\text{m}$) 的 R1233zd 液膜分别进行了 10 次重复性测量, 结果如图 4(a) 所示, 其中板间距离为已知的液膜厚度。10 次重复性实验的液膜厚度测量值的标准差如图 4(b) 所示, 可以看出, 在已知厚度为 $800 \text{ }\mu\text{m}$ 时标准差最大, 为 $0.5 \text{ }\mu\text{m}$ 。液膜厚度测量值与已知值的平均相对偏差为 1.0% 。其中, 当已知厚度为 $600 \text{ }\mu\text{m}$ 时相对偏差最大, 为 0.8% 。由此可见, 该系统能够实现制冷剂液膜厚度的高精度测量。

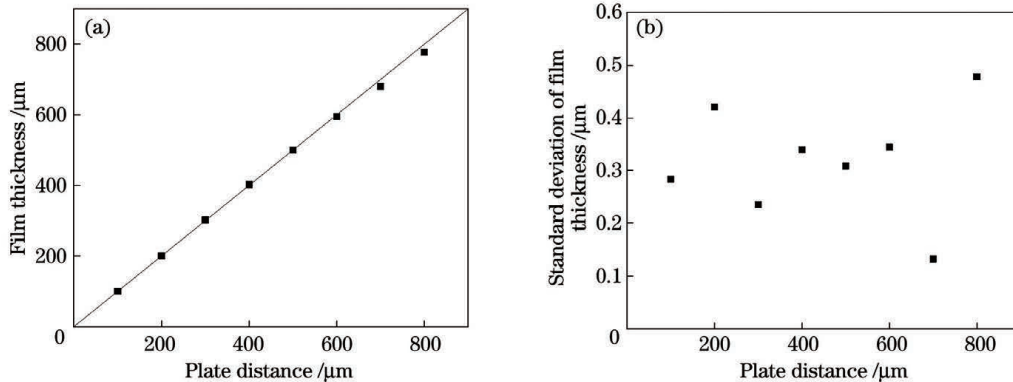


图4 液膜厚度测量结果。(a) 测量的液膜厚度与已知的液膜厚度的对比; (b) 薄膜厚度的标准差

Fig. 4 Measurement results of film thicknesses. (a) Comparison of measured and known film thicknesses; (b) standard deviation of film thickness

3.2 水平石英玻璃板上 R1233zd 液膜蒸发过程的研究

在此基础上, 利用该测量系统对水平透明石英玻璃圆板 (直径 $\phi = 100.0 \text{ mm}$) 上 R1233zd 的液膜蒸发过程进行研究。首先使用胶头滴管布液, 制备一定初始厚度的液膜, 同时结合图像法进行同步验证, 测量装置如图 5 所示, 吸收光谱法的光路布置与图 3 相同, 白

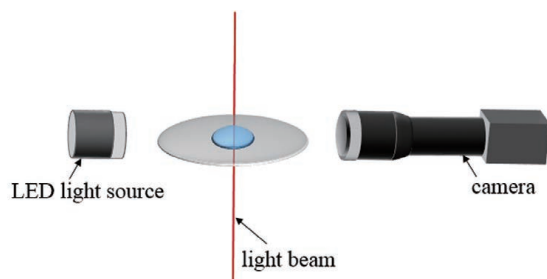


图5 水平石英玻璃板上 R1233zd 液膜蒸发过程研究的实验装置图

Fig. 5 Experimental setup for investigating R1233zd film evaporation process on quartz plate

光光束与水平石英玻璃板表面垂直。图像法采用发光二极管 (LED) 作为背景光源, 通过电荷耦合器件 (CCD) 相机采集液膜图片。CCD 相机与吸收光谱法测点的距离保持为 110 mm (焦距), LED 与 CCD 相机中心连线和水平石英板表面平行, 确保相机能够捕捉到测点处的清晰图像。对于图像法, 首先对获取的液膜图像进行灰度化预处理, 同时基于原始背景图像进行差影检测, 进一步通过中值滤波滤除噪声干扰, 使用 Otsu 阈值分割算法对图像进行分割识别, 准确提取液膜图像厚度信息。

图 6 为水平石英玻璃板表面上 R1233zd 液膜蒸发过程中膜厚随时间的变化情况。可以看出, 吸收光谱法和图像法测得的液膜的初始厚度分别为 $410.8 \text{ }\mu\text{m}$ 和 $409.7 \text{ }\mu\text{m}$, 相对偏差为 0.26% 。随着液膜蒸发过程的进行, 两种方法测得的液膜厚度变化趋势基本一致, 平均相对偏差均为 1.1% 。吸收光谱法能够追踪整个蒸发过程中液膜厚度的变化情况, 而液膜厚度低于 $50 \text{ }\mu\text{m}$ 时, 由于图像对比度太低, 图像法

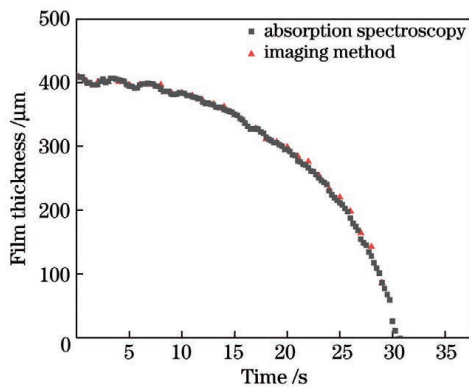


图6 R1233zd液膜蒸发过程中膜厚随时间的变化情况

Fig. 6 Thickness versus time during evaporation process of R1233zd films

无法获取液膜厚度信息。

利用图像法处理液膜蒸发过程(图6)中6个特定时刻(0, 6.0, 12.0, 18.0, 24.0, 30.0 s)的图像,结果如图7所示。其中,白色水平线表示石英玻璃板和液膜的分界面,分界面上侧为液膜,时刻 t_1 图像中白点表示吸收光谱法的测点。 $t_1 \sim t_2$ 为蒸发过程的初期,液膜蒸发缓慢,膜厚变化较小; $t_3 \sim t_4$ 为蒸发过程的中期,液膜蒸发相对迅速,吸收光谱法和图像法测得的液膜厚度变化率分别为 $11.6 \mu\text{m/s}$ 和 $11.5 \mu\text{m/s}$ 。这是由于液膜边缘较薄,蒸发迅速完成,液体收缩汇聚到液膜中心,测点位置液体蒸发的效果大于周围液体汇聚的效果。 $t_5 \sim t_6$ 为蒸发过程的后期,液膜厚度迅速减小。这是由于在液膜蒸发后期,没有多余的液体收缩汇聚到中心位置。

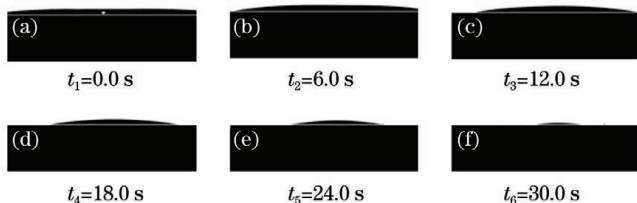


图7 经图像法处理的液膜蒸发过程中6个特定时刻的图像

Fig. 7 Processed images at six specific moments during liquid film evaporation process by imaging method

4 结 论

以R1233zd为研究对象,提出了一种具有普适性的制冷剂液膜厚度测量新方法。首先结合自制的高精度温度控制装置和高分辨率的傅里叶红外变换光谱仪,获取了不同温度下R1233zd的吸收光谱。在此基础上,构建了制冷剂液膜厚度反演模型,并研制了基于吸收光谱技术的R1233zd液膜厚度测量系统。利用液膜厚度可调(0~800 mm)的标准具对该系统的测量精度进行验证,发现该系统液膜厚度测量的平均误差为1.0%。结合图像法对水平石英玻璃板上的R1233zd蒸发过程进行研究,发现吸收光谱法能够追踪整个蒸发过程中液膜厚度的变化情况。该方法也适

用于其他种类的制冷剂,具有结构紧凑、操作简单等优点,能够实现液膜厚度的无干扰和高精度测量。可同时获取宽波段光谱信息,有利于后期研究中温度等其他参数的确定,有望为相关工业过程的设计和 optimization 提供测试手段和数据支撑。

参 考 文 献

- [1] 卢杏斌. 制冷剂竖管降膜蒸发的流动与换热特性研究[D]. 广州: 华南理工大学, 2020: 1-6.
Lu X B. Research on heat and flow characteristic of falling film evaporation of refrigerant on vertical tube [D]. Guangzhou: South China University of Technology, 2020: 1-6.
- [2] 吕坤鹏, 刘震宇, 杨雪, 等. 高功率固体激光器微通道冷却结构的数值研究[J]. 中国激光, 2020, 47(6): 0601010.
Lü K P, Liu Z Y, Yang X, et al. Numerical research on microchannel cooling structure of high power solid-state lasers [J]. Chinese Journal of Lasers, 2020, 47(6): 0601010.
- [3] 蒋琳, 刘军, 袁晓蓉, 等. 薄片激光器低畸变冷却技术研究[J]. 中国激光, 2021, 48(3): 0301001.
Jiang L, Liu J, Yuan X R, et al. Cooling techniques for deformation reduction of thin-disk lasers [J]. Chinese Journal of Lasers, 2021, 48(3): 0301001.
- [4] Lee S, Mudawar I. Investigation of flow boiling in large micro-channel heat exchangers in a refrigeration loop for space applications [J]. International Journal of Heat and Mass Transfer, 2016, 97: 110-129.
- [5] 田华, 程彬, 马一太, 等. 制冷空调系统水平管降膜蒸发研究[J]. 制冷与空调, 2011, 11(4): 103-110.
Tian H, Cheng B, Ma Y T, et al. Research on falling film evaporation on horizontal tubes of refrigeration and air-conditioning system [J]. Refrigeration and Air-Conditioning, 2011, 11(4): 103-110.
- [6] Zhao C Y, Ji W T, Jin P H, et al. Effect of downward vapor stream on falling film evaporation of R134a in a tube bundle [J]. International Journal of Refrigeration, 2018, 89: 112-121.
- [7] 孙少鹏. 高热流密度电子元件喷雾相变冷却系统的研究[D]. 重庆: 重庆大学, 2010: 1-13.
Sun S P. Research on spray cooling system for electronics with high heat flux [D]. Chongqing: Chongqing University, 2010: 1-13.
- [8] Lin S, Liu X, Li X L. The spatial distribution of liquid film thickness outside the horizontal falling film tube [J]. International Journal of Heat and Mass Transfer, 2019, 143: 118577.
- [9] 章曦, 李平雪, 董雪岩, 等. 万瓦级光纤连接器参数设计及热效应数值模拟[J]. 激光与光电子学进展, 2021, 58(1): 0114009.
Zhang X, Li P X, Dong X Y, et al. Parameter design and thermal effect numerical simulation of 10 kW fiber connector [J]. Laser & Optoelectronics Progress, 2021, 58(1): 0114009.
- [10] Li W, Lyu D, Zhang J Z, et al. Condensation heat transfer and flow properties of R134a refrigerant in rectangular minichannel: a numerical study [J]. Journal of Thermal Science and Engineering Applications, 2020, 12(2): 021006.
- [11] 蒋淳, 陈振乾. 水平管外降膜蒸发流动和传热特性数值模拟[J]. 化工学报, 2018, 69(10): 4224-4230.
Jiang C, Chen Z Q. Numerical simulation of fluid flow and heat transfer characteristics of falling film evaporation outside horizontal tubes [J]. CIESC Journal, 2018, 69(10): 4224-4230.
- [12] Sripattaran W, Wongchang T, Wongwiset S. Heat transfer and two-phase flow characteristics of refrigerants flowing under varied heat flux in a double-pipe evaporator [J]. Heat and Mass Transfer, 2004, 40(8): 653-664.
- [13] 王宇辰, 陈建业, 徐璐, 等. 基于电容法的管内低温流体液膜厚度测量方法[J]. 浙江大学学报(工学版), 2016, 50(10): 1855-1858.

- Wang Y C, Chen J Y, Xu L, et al. Permittivity-based liquid film sensor for cryogenic fluid[J]. *Journal of Zhejiang University (Engineering Science)*, 2016, 50(10): 1855-1858.
- [14] Wang R L, Lee B A, Lee J S, et al. Analytical estimation of liquid film thickness in two-phase annular flow using electrical resistance measurement[J]. *Applied Mathematical Modelling*, 2012, 36(7): 2833-2840.
- [15] Yu Y X, Ma L, Ye H Y, et al. Design of instantaneous liquid film thickness measurement system for conductive or non-conductive fluid with high viscosity[J]. *AIP Advances*, 2017, 7(6): 065207.
- [16] Wang M, Zheng D D, Xu Y. A new method for liquid film thickness measurement based on ultrasonic echo resonance technique in gas-liquid flow [J]. *Measurement*, 2019, 146: 447-457.
- [17] Zhang K, Dou P, Wu T H, et al. An ultrasonic measurement method for full range of oil film thickness[J]. *Proceedings of the Institution of Mechanical Engineers, Part J: Journal of Engineering Tribology*, 2019, 233(3): 481-489.
- [18] 杨荟楠, 郭晓龙, 苏明旭, 等. 基于 TDLAS 技术在线测量气流道内液膜动态厚度[J]. *中国激光*, 2014, 41(12): 1208010. Yang H N, Guo X L, Su M X, et al. Liquid-water film-thickness online measurement in a flow channel by TDLAS[J]. *Chinese Journal of Lasers*, 2014, 41(12): 1208010.
- [19] de Oliveira F S, Yanagihara J I, Pacifico A L. Film thickness and wave velocity measurement using reflected laser intensity [J]. *Journal of the Brazilian Society of Mechanical Sciences and Engineering*, 2006, 28(1): 30-36.
- [20] Youn Y J, Han Y, Shikazono N. Liquid film thicknesses of oscillating slug flows in a capillary tube [J]. *International Journal of Heat and Mass Transfer*, 2018, 124: 543-551.
- [21] Ye X, Hao T T, Chen Y S, et al. Liquid film transport around Taylor bubble in a microchannel with gas cavities[J]. *Chemical Engineering and Processing-Process Intensification*, 2020, 148: 107828.
- [22] Klausner J F, Zeng L Z, Bernhard D M. Development of a film thickness probe using capacitance for asymmetrical two-phase flow with heat addition [J]. *Review of Scientific Instruments*, 1992, 63(5): 3147-3152.
- [23] Vergne P, Fillot N, Bouscharain N, et al. An experimental and modeling assessment of the HCFC-R123 refrigerant capabilities for lubricating rolling EHD circular contacts[J]. *Proceedings of the Institution of Mechanical Engineers, Part J: Journal of Engineering Tribology*, 2015, 229(8): 950-961.
- [24] Martínez-Galván E, Ramos J C, Antón R, et al. Film thickness and heat transfer measurements in a spray cooling system with R134a [J]. *Journal of Electronic Packaging*, 2011, 133(1): 011002.
- [25] Ko J W, Jeon D S, Kim Y L, et al. Experimental study on film condensation heat transfer characteristics of R1234ze(E) and R1233zd(E) over horizontal plain tubes [J]. *Journal of Mechanical Science and Technology*, 2018, 32(1): 527-534.

Development of Measurement System of Refrigerant Film Thickness Based on Absorption Spectroscopy

Kong Shuaishuai, Xu Xiaoyan, Sun Hao, Fang Yidong, Su Mingxu, Yang Huinan*

School of Energy and Power Engineering, University of Shanghai for Science and Technology, Shanghai 200093, China

Abstract

Objective The evaporation of refrigerant films is common in aviation and aerospace, refrigeration and air-conditioning, and other industries. Film thickness measurement helps understand the heat transfer mechanisms of liquid films during the formation, flow, and evaporation processes. Several researchers have worked on numerical simulations of refrigerant films. However, because numerical simulations are often based on simplified assumptions, the simulation results are less credible. Meanwhile, a large number of experiments on the measurement of liquid film thickness have been performed using various methods, including electrical, acoustic, and optical methods, but the work relevant to refrigerant films is relatively limited. The capacitive method, optical interferometry, and imaging method have been used to investigate the refrigerant liquid film. However, the above-mentioned methods have certain limitations. Measurement of refrigerant film thickness cannot be performed with high accuracy. Therefore, a novel refrigerant film thickness measurement system based on absorption spectroscopy is proposed. It demonstrates that high-accuracy thickness measurement is possible. This system can provide scientific guidance for the design and optimization of relevant industrial devices and processes.

Methods In the study, R1233zd is used as the refrigerant. The absorption spectra in the near-infrared region ($5800.0\text{--}6300.0\text{ cm}^{-1}$) of R1233zd at different temperatures (11.8, 13.5, 15.2, 16.5, 18.0 °C) below the boiling point are measured using a self-designed temperature control device with high precision and a Fourier-transform infrared spectrometer with high resolution (Fig. 2). Based on the Beer-Lambert law, two wavenumber positions (ν_1 and ν_2) are chosen to eliminate the influence of light intensity attenuation caused by other factors. The absorption coefficient is significant at ν_1 and close to zero at ν_2 . The absorption coefficients at these two wavenumber positions should be nearly temperature independent. An inversion model is developed, which is also applicable to other refrigerants.

Results and Discussions The measurement system is developed based on absorption spectroscopy. The system's measurement accuracy is validated using a calibration tool with known film thicknesses (0–800 μm). Eight different film thicknesses (100, 200, 300, 400, 500, 600, 700, 800 μm) are measured ten times. The largest standard deviation of film thickness for the ten repeated experiments is 0.5 μm when the known thickness is 800 μm . Moreover, the average

relative deviation between the measured and known thickness is 1.0%. This demonstrates that the system can achieve high accuracy in measuring refrigerant film thickness. Furthermore, the processes of R1233zd film evaporation on a horizontal transparent quartz plate are investigated. In this case, the imaging method is used as a comparison method. To ensure clear images, the distance between the measuring point of the absorption spectroscopy and the camera is kept at 110 mm (i.e., the focal length of the camera). The obtained liquid film image is processed, and the liquid film thickness can be accurately determined. The initial film thicknesses obtained using absorption spectroscopy and imaging method are 410.8 μm and 409.7 μm , respectively. The relative deviations in thickness measured using the two methods are 0.26%. It is discovered that the film thickness variations measured using the two methods are similar during the evaporation processes, with average relative deviations of 1.1%. The absorption spectroscopy can also be used to track the changes in film thickness throughout the evaporation process. However, the imaging method is not available due to its contrast ratio limitation when the film thickness is less than 50 μm . The liquid film evaporates slowly at the beginning of the evaporation process and the film thickness changes little. The effect of liquid evaporation is more significant than that of liquid shrinkage at the measuring point in the middle of the evaporation process. The thickness of the liquid film decreases rapidly later in the evaporation process. There is no excess liquid converging to the liquid film's central position.

Conclusions In this work, a novel refrigerant film thickness measurement system is developed by absorption spectroscopy. An inversion model is established to determine film thicknesses. The measurement accuracy of the system is validated by a calibration tool. Furthermore, the R1233zd film evaporation processes are investigated. The system can measure liquid film thicknesses noninvasively and with high accuracy, and it is also suitable for other refrigerant types. It has the advantages of a compact structure and simple operation. Wide-band spectral information can be obtained using this system, which will be useful for determining temperature and other parameters in future research.

Key words measurement; absorption spectroscopy; film thickness; evaporation